Electronic Supplementary Material (ESI) for Dalton Transactions.

Reversible uptake of sulfur-containing gases by single crystals of a Cr8 metallacrown

Iñigo J. Vitórica-Yrezábal*, Daniel Florin Sava, Daniel Reta, Grigore A. Timco and Richard E.P. Winpenny*

Supporting Information

S1. Synthesis

Synthetic details

Unless stated otherwise, all reagents and solvents were purchased from Sigma Aldrich Chemicals and used without further purification.

Synthesis of $[Cr_8(\mu\text{-}F)_8(O_2C\text{-}^tBu)_{16}]$ (**Cr_8**) was reported in a previous study.[1] All the **Cr_8** crystals used in these experiments are from the same batch. ESI-MS (m/z): + 2207 $[M + Na]^+$ (100%); Elem. Anal. (calc./exp.): C (43.96/44.07), H (6.64/6.68) and Cr (19.03/19.05).

Synthesis of $[Cr_8(\mu\text{-}F)_8(O_2C\text{-}^tBu)_{16}]\cdot 0.849SO_2$ –**SO_2@Cr_8**

Crystals of **Cr_8** were placed in a flask which was purged with SO_2 from the reaction between $NaHSO_3/Na_2S_2O_5$ and H_2SO_4. The produced gas was passed through a drying ($CaCl_2$) column before purging the crystals. Elem. Anal. (calc./exp.): C (42.91/43.31), H (6.48/6.61), S(1.21/0.88) and Cr (18.58/18.62). TGA – loses 2.5089% between 42.97 and 262.4°C which corresponds to 0.878 SO_2

Synthesis of $[Cr_8(\mu\text{-}F)_8(O_2C\text{-}^tBu)_{16}]\cdot 0.787\ H_2S$ – **H_2S@Cr_8**

Crystals of **Cr_8** were placed in a flask which was purged with H_2S from the reaction between FeS and HCl. The produced gas was passed through a drying ($CaCl_2$) column before purging the crystals. Elem. Anal. (calc./exp.): C (43.44/43.89), H (6.56/6.73), S(1.14/0.68) and Cr (18.80/18.08). TGA – loses 1.6601% between 56.5 and 271.3°C which corresponds to 1.15 H_2S.

S2. FTIR spectra

FTIR studies were carried out on a Thermo Scientific™ Nicolet™ iS™5 FT-IR with an iD5 ATR Accessory working in the range of 600-4000 cm^{-1}. Each spectrum was obtained as an average of 16 individual scans, at a resolution of 4 cm^{-1}.

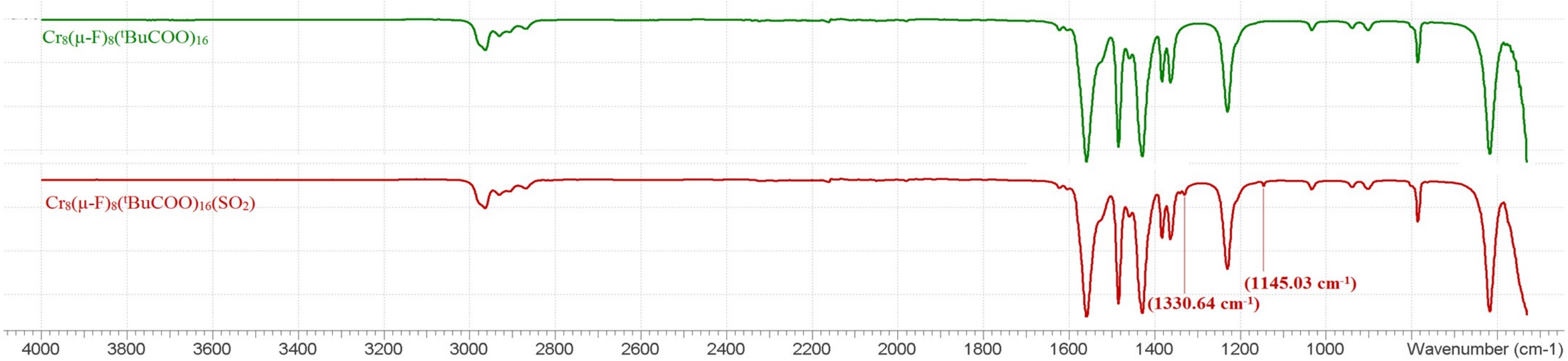

Figure S1. FTIR spectra of $\mathbf{Cr_8}$ and $\mathbf{SO_2@Cr_8}$

S3. Thermogravimetric analysis

TGA analysis for compounds **SO_2@Cr_8 and H_2S@Cr_8** were done in a Perkin-Elmer instrument. The samples were heated at 5°C/minute from room temperature to 600°C under a flow of dry nitrogen gas.

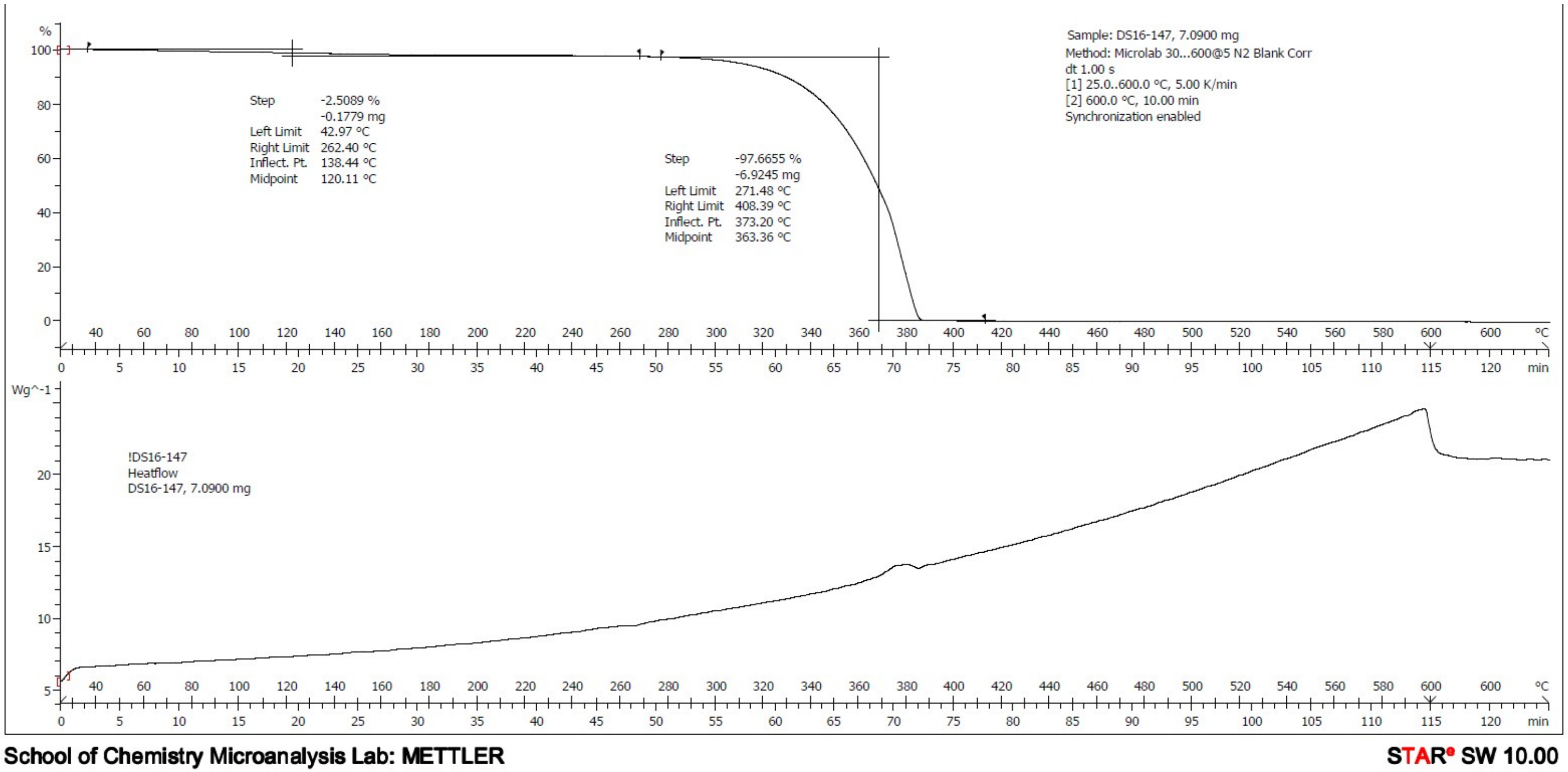

Figure S2. TGA of **SO_2@Cr_8**

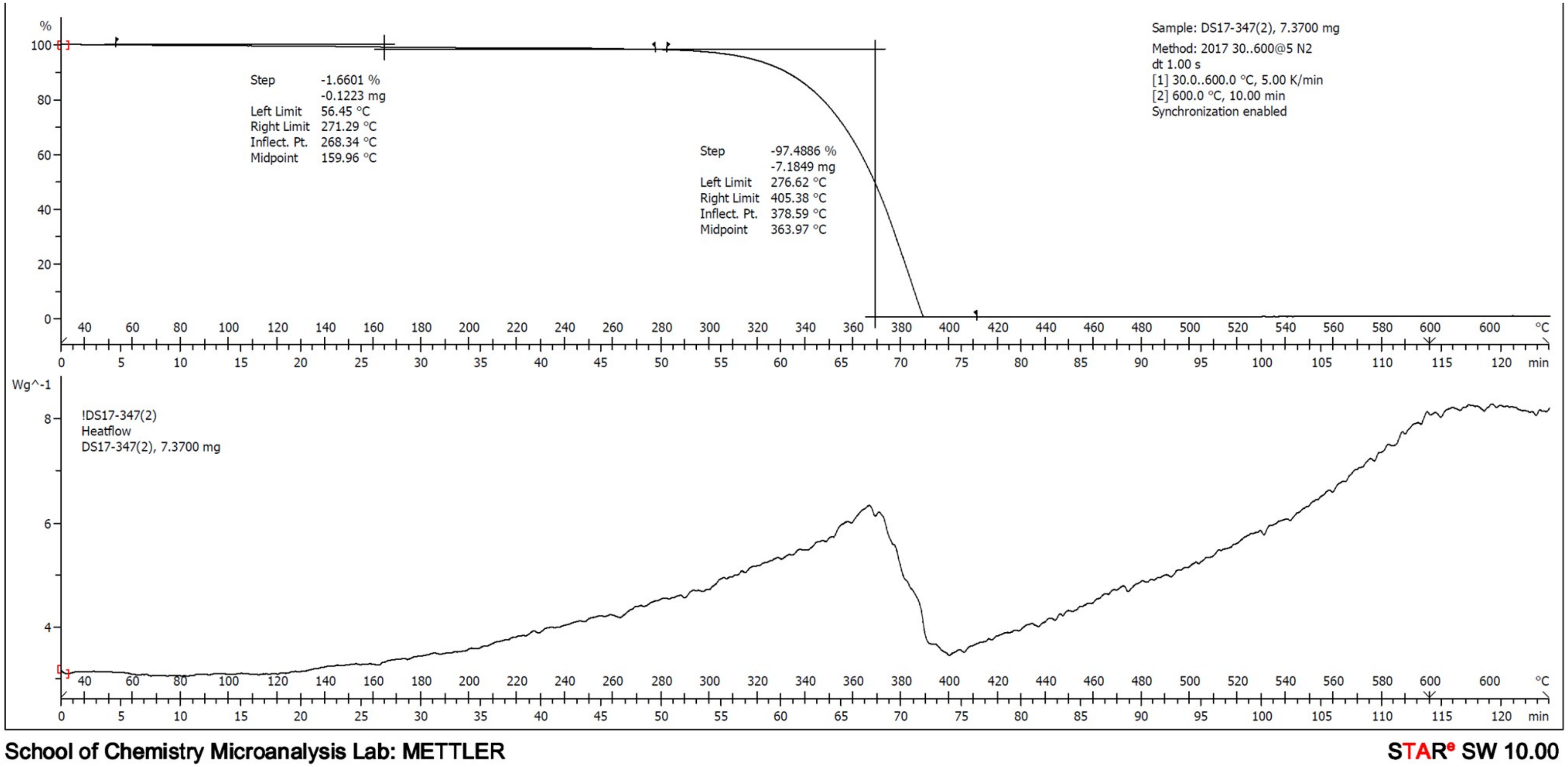

Figure S3. TGA of **$H_2S@Cr_8$**

S4. DSC analysis

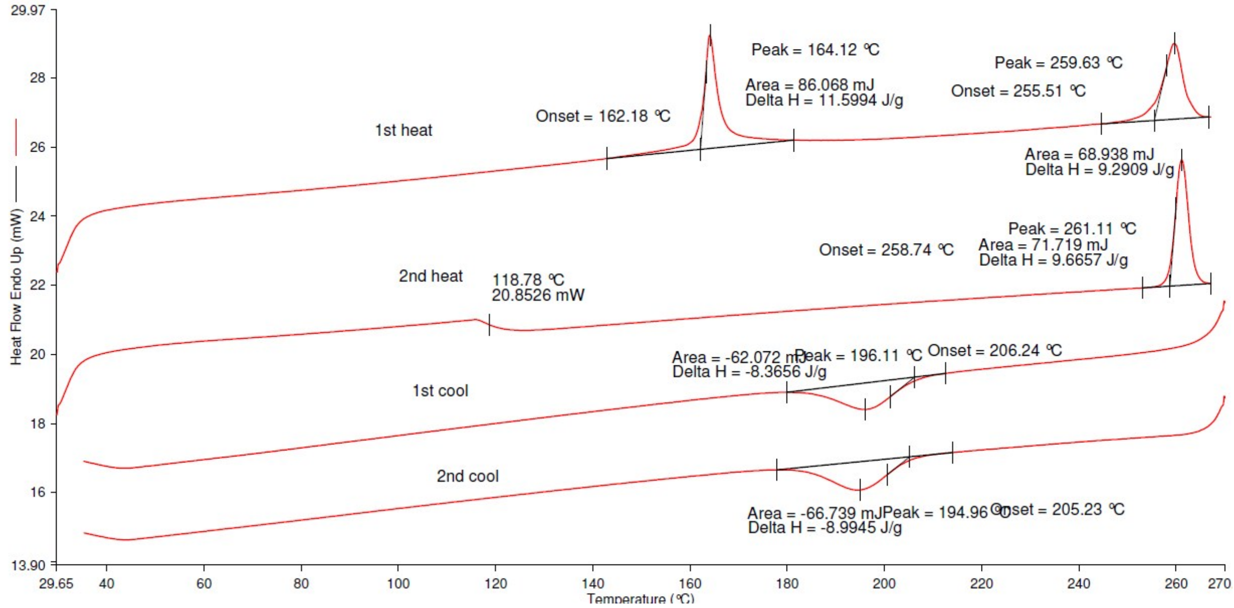

Figure S4. DSC of $\mathbf{SO_2@Cr_8}$

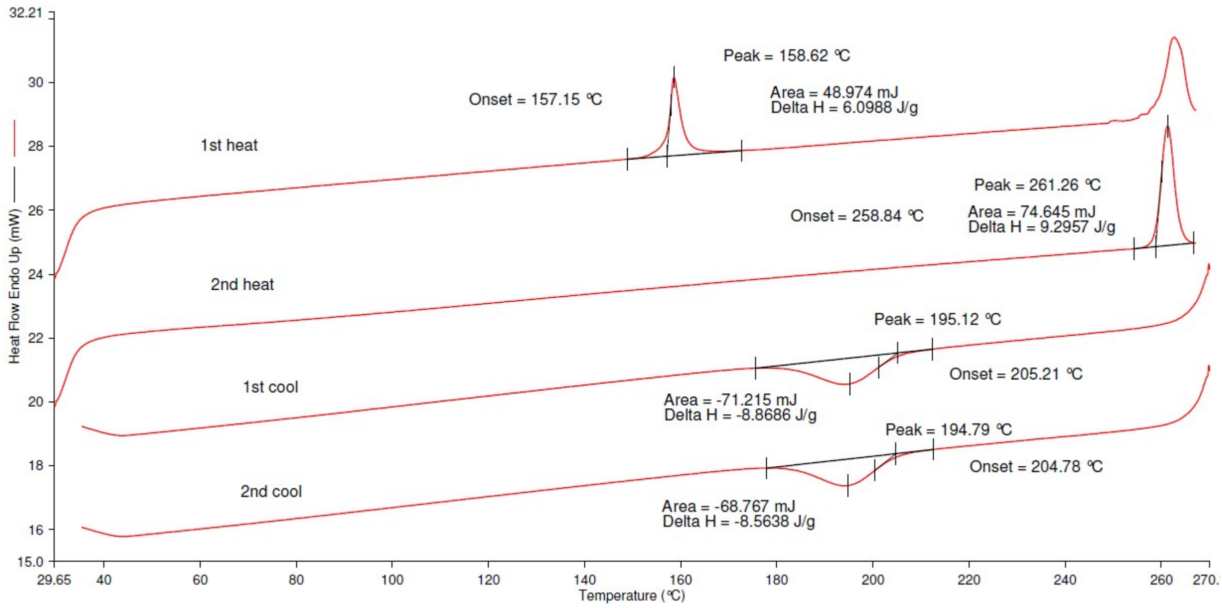

Figure S5. TGA of $\mathbf{H_2S@Cr_8}$

S5. Single crystal X-ray diffraction

Data Collection.

Single crystal X-ray diffraction data were collected for the crystal structures **SO_2@Cr_8_100K**, **SO_2@Cr_8_150K**, **SO_2@Cr_8_200K**, **SO_2@Cr_8_250K** and **SO_2@Cr_8_VT350K_1-7** (240K) at a using Mo-Kα radiation (λ = 0.71073 Å) on an Agilent Supernova, equipped with an Oxford Cryosystems Cobra nitrogen flow gas system and

Single crystal X-ray diffraction data were collected for the crystal structures **H_2S@Cr_8** (100K), **H_2S@Cr_8_VT350K_1-2** (240K), **SO_2@Cr_8_300K**, **SO_2@Cr_8_310K**, **SO_2@Cr_8_350K** , **SO_2@Cr_8_VT400K_1-2** (240K), **SO_2@Cr_8_hkl_400K** (150K), **SO_2@Cr_8_hkl_375K** (150K), and **SO_2@Cr_8_hkl_350K** (150K) on a Rigaku FR-X diffractometer with a HyPix 6000HE detector and microfocus optics with Mo Kα radiation (λ = 0.71073 Å). Data were measured using CrysAlisPro suite of programs.

SO_2@Cr_8_100-250K is a set of variable temperature experiments where single crystal X-ray diffraction data were collected at 100K, 150K, 200K and 250K on the same crystal.

SO_2@Cr_8_300-350K is a second set of variable temperature experiments where single crystal X-ray diffraction data were collected at 300, 310 and 350K on the same crystal

VT350K_1-7 – is a heating experiment where Single crystal X-ray diffraction data were collected at 240 K, and then the crystal was heated up to 350K where it was kept for one hour, before the temperature was decreased at 240 K for another collection. (This cycles was repeated up to 6 times)

VT400K – is a heating experiment where Single crystal X-ray diffraction data were collected at 240 K, and then the crystal was heated up to 400K where it was kept for three hours, before the temperature was decreased at 240 K for another collection.

hkl(400, 375 or 350K) – is a series of experiments where the SO_2 release was studied by monitoring the change in the intensity of two reflexions ((110) and (11-2)). In all three experiments, an initial full data collection was under 150 K to confirm the presence of **SO_2@Cr_8**. Then, crystals were heated to 350, 375 and 400 K respectively, where short data collections were undertaken for eight (350K), four (375K) and two (400K) hours.

Crystal structure determinations and refinements.

X-ray data were processed and reduced using CrysAlisPro suite of programs for crystals. Absorption correction was performed using empirical methods based upon symmetry-equivalent reflections combined with measurements at different azimuthal angles using SCALE3 ABSPACK. The crystal structures were solved and refined against all F^2 values using the SHELX and Olex2 suite of programs[2,3]. All the non-hydrogen atoms were refined anisotropically. Hydrogen atoms were placed in calculated positions and refined using idealized geometries (riding model) and assigned fixed isotropic displacement parameters. Pivalate ligands in all the crystal structures were disordered and modelled over two positions where possible. SHELX SADI, and DFIX commands were used to restrain the C-C bonds. SIMU and RIGU commands were used to restrain the atomic displacement parameters.

SO_2 molecule is described as disordered over 3 positions, with sulphur and oxygen atoms modelled using SADI and DFIX bond distance restrain commands. The occupancies of the three component disorder of the SO_2 molecules has been modelled and refined without using any restrain. An independent variable was defined for each component of the SO_2 disorder, and the value were allowed to refine freely. The atomic displacement parameters (adp) of the SO_2 model have been restrained using RIGU and SIMU commands.

High angle data was collected to allow a diffraction limit of 0.5 Angstroms, thus having a better accuracy of the hydrogen atoms position. Sulphur atom has 3 regions of electron density in the difference map which could be identify as hydrogens. H_2S molecule was modelled as a two part disorder, where the H_2S molecules were rotated 180° respect each other. Sulphur and hydrogen atoms were modelled using SADI and DFIX bond distance restrain commands. An independent variable was defined for each component of the H_2S disorder, and the value were allowed to refine freely.

CCDC 1920753-1920774 contains the supplementary crystallographic data for this paper. These data can be obtained free of charge via www.ccdc.cam.ac.uk/conts/retrieving.html (or from the Cambridge Crystallographic Data Centre, 12 Union Road, Cambridge CB21EZ, UK; fax: (+44)1223-336-033; or deposit@ccdc.cam.ac.uk. Diamond and POV-Ray software packages were used for graphical images.

Table S1. Crystallographic information for $\mathbf{H_2S@Cr_8}$, **$\mathbf{H_2S}$@Cr8_VT350K_1** and **$\mathbf{H_2S}$@Cr8_VT350K_2**

Identification code	$\mathbf{H_2S@Cr_8}$	**$\mathbf{H_2S}$@Cr8_VT350K_1**	**$\mathbf{H_2S}$@Cr8_VT350K_2**
Empirical formula	$C_{80}H_{145.57}Cr_8F_8O_{32}S_{0.78}$	$C_{80}H_{145.3}Cr_8F_8O_{32}S_{0.67}$	$C_{80}H_{144}Cr_8F_8O_{32}$
Formula weight	2212.69	2208.57	2185.94
Temperature/K	100.0	239.98(10)	239.92(10)
Crystal system	monoclinic	monoclinic	monoclinic
Space group	I2/a	I2/a	I2/a
a/Å	34.8280(4)	34.7389(9)	34.7353(9)
b/Å	16.46848(17)	16.5853(4)	16.5967(4)
c/Å	43.7202(6)	44.6977(13)	44.7645(14)
α/°	90	90	90
β/°	111.3334(15)	111.333(3)	111.279(3)
γ/°	90	90	90
Volume/Å^3	23358.1(5)	23988.3(12)	24047.0(12)
Z	8	8	8
ρ_{calc}g/cm^3	1.258	1.223	1.208
μ/mm^{-1}	0.806	0.782	0.769
F(000)	9265.0	9248.0	9152.0
Crystal size/mm^3	0.2 × 0.2 × 0.1	0.4 × 0.1 × 0.1	0.4 × 0.1 × 0.1
Radiation	MoKα (λ = 0.71073)	MoKα (λ = 0.71073)	MoKα (λ = 0.71073)
2Θ range for data collection/°	4.478 to 90.588	3.396 to 53.464	3.886 to 52.742
Index ranges	$-69 \le h \le 69$, $-22 \le k \le 32$, $-87 \le l \le 86$	$-43 \le h \le 43$, $-12 \le k \le 20$, $-56 \le l \le 53$	$-43 \le h \le 43$, $-12 \le k \le 20$, $-53 \le l \le 55$
Reflections collected	322797	69870	68925
Independent reflections	97655 [R_{int} = 0.0420, R_{sigma} = 0.0540]	25333 [R_{int} = 0.0229, R_{sigma} = 0.0312]	24550 [R_{int} = 0.0241, R_{sigma} = 0.0329]
Data/restraints/parameters	97655/293/1330	25333/804/1484	24550/801/1463
Goodness-of-fit on F^2	1.007	1.012	1.041
Final R indexes [I>=2σ (I)]	R_1 = 0.0460, wR_2 = 0.1071	R_1 = 0.0516, wR_2 = 0.1281	R_1 = 0.0515, wR_2 = 0.1466
Final R indexes [all data]	R_1 = 0.0901, wR_2 = 0.1235	R_1 = 0.0717, wR_2 = 0.1384	R_1 = 0.0748, wR_2 = 0.1603
Largest diff. peak/hole / e Å^{-3}	1.31/-0.84	0.53/-0.62	1.19/-0.54

Table S2. Crystallographic information for **SO_2@Cr_8_100K, SO_2@Cr_8_150K, SO_2@Cr_8_200K** and **SO_2@Cr_8_250K**

Identification code	**SO_2@Cr_8_100K**	**SO_2@Cr_8_150K**	**SO_2@Cr_8_200K**	**SO_2@Cr_8_250K**
Empirical formula	$C_{80}H_{144}Cr_8F_8O_{33.74}S_{0.87}$	$C_{80}H_{144}Cr_8F_8O_{33.73}S_{0.87}$	$C_{80}H_{144}Cr_8F_8O_{33.76}S_{0.88}$	$C_{80}H_{144}Cr_8F_8O_{33.76}S_{0.88}$
Formula weight	2241.66	2241.44	2242.42	2242.42
Temperature/K	100	149.8(5)	200	249.9(5)
Crystal system	Monoclinic	monoclinic	monoclinic	monoclinic
Space group	I2/a	I2/a	I2/a	I2/a
a/Å	34.9320(7)	34.8985(11)	34.8857(11)	34.9090(12)
b/Å	16.4600(3)	16.5023(4)	16.5618(4)	16.6118(4)
c/Å	43.7453(11)	44.0954(16)	44.4679(17)	44.8078(18)
α/°	90	90	90	90
β/°	111.406(3)	111.428(4)	111.459(4)	111.483(5)
γ/°	90	90	90	90
Volume/Å^3	23417.6(10)	23639.4(14)	23911.2(15)	24178.9(16)
Z	8	8	8	8
ρ_{calc}g/cm^3	1.272	1.260	1.246	1.232
μ/mm^{-1}	0.807	0.799	0.791	0.782
F(000)	9375.0	9374.0	9378.0	9378.0
Crystal size/mm^3	0.5 × 0.1 × 0.1	0.5 × 0.1 × 0.1	0.5 × 0.1 × 0.1	0.5 × 0.1 × 0.1
Radiation	MoKα (λ = 0.71073)	MoKα (λ = 0.71073)	MoKα (λ = 0.71073)	MoKα (λ = 0.71073)
2Θ range for data collection/°	6.564 to 52.744	6.556 to 52.744	6.546 to 52.744	6.47 to 52.744
Index ranges	$-43 \le h \le 43$, $-20 \le k \le 20$, $-39 \le l \le 54$	$-43 \le h \le 43$, $-20 \le k \le 20$, $-55 \le l \le 40$	$-43 \le h \le 43$, $-20 \le k \le 20$, $-55 \le l \le 40$	$-43 \le h \le 43$, $-20 \le k \le 20$, $-55 \le l \le 40$
Reflections collected	58905	59475	60498	61003
Independent reflections	23866 [R_{int} = 0.0573, R_{sigma} = 0.0875]	24082 [R_{int} = 0.0604, R_{sigma} = 0.0937]	24400 [R_{int} = 0.0560, R_{sigma} = 0.0931]	24666 [R_{int} = 0.0618, R_{sigma} = 0.1061]
Data/restraints/parameters	23866/701/1433	24082/729/1461	24400/845/1486	24666/977/1536
Goodness-of-fit on F^2	1.042	1.036	1.029	1.031
Final R indexes [I>=2σ (I)]	R_1 = 0.0593, wR_2 = 0.1178	R_1 = 0.0596, wR_2 = 0.1242	R_1 = 0.0647, wR_2 = 0.1404	R_1 = 0.0703, wR_2 = 0.1558
Final R indexes [all data]	R_1 = 0.0935, wR_2 = 0.1334	R_1 = 0.1036, wR_2 = 0.1478	R_1 = 0.1186, wR_2 = 0.1706	R_1 = 0.1409, wR_2 = 0.1972
Largest diff. peak/hole / e Å^{-3}	0.99/-0.93	0.68/-0.70	0.78/-0.55	0.58/-0.49

Table S3. Crystallographic information for **SO_2@Cr_8_300K, SO_2@Cr_8_310K** and **SO_2@Cr_8_350K**

Identification code	**SO_2@Cr_8_300K**	**SO_2@Cr_8_310K**	**SO_2@Cr_8_350K**
Empirical formula	C80H144Cr8F8O33.68S0.84	$C_{80}H_{144}Cr_8F_8O_{33.58}S_{0.79}$	$C_{80}H_{144}Cr_8F_8O_{33.27}S_{0.64}$
Formula weight	2239.77	2236.41	2226.78
Temperature/K	300(5)	310.00(10)	350.02(10)
Crystal system	Monoclinic	monoclinic	monoclinic
Space group	I2/a	I2/a	I2/a
a/Å	34.9677(13)	34.8686(15)	34.8127(17)
b/Å	16.6698(3)	16.6607(6)	16.6793(8)
c/Å	45.0674(18)	45.0570(19)	45.240(2)
α/°	90	90	90
β/°	111.330(4)	111.276(5)	111.106(6)
γ/°	90	90	90
Volume/Å3	24470.6(16)	24391.2(19)	24506(2)
Z	8	8	8
ρcalcg/cm3	1.216	1.218	1.207
μ/mm-1	0.772	0.773	0.767
F(000)	9367.0	9354.0	9315.0
Crystal size/mm3	0.5 × 0.25 × 0.1	0.5 × 0.25 × 0.1	0.5 × 0.25 × 0.1
Radiation	MoKα (λ = 0.71073)	MoKα (λ = 0.71073)	MoKα (λ = 0.71073)
2Θ range for data collection/°	3.376 to 52.744	3.616 to 52.746	3.606 to 52.746
Index ranges	-43 ≤ h ≤ 43, -17 ≤ k ≤ 20, -56 ≤ l ≤ 39	-43 ≤ h ≤ 38, -17 ≤ k ≤ 20, -54 ≤ l ≤ 56	-43 ≤ h ≤ 38, -17 ≤ k ≤ 20, -54 ≤ l ≤ 56
Reflections collected	75160	62308	62677
Independent reflections	24771 [Rint = 0.0461, Rsigma = 0.0649]	24735 [R_{int} = 0.0373, R_{sigma} = 0.0600]	24857 [R_{int} = 0.0438, R_{sigma} = 0.0725]
Data/restraints/parameters	24771/983/1536	24735/989/1536	24857/1031/1536
Goodness-of-fit on F2	1.035	1.046	1.040
Final R indexes [I>=2σ (I)]	R1 = 0.0596, wR2 = 0.1589	R_1 = 0.0611, wR_2 = 0.1662	R_1 = 0.0657, wR_2 = 0.1784
Final R indexes [all data]	R1 = 0.1148, wR2 = 0.1847	R_1 = 0.1144, wR_2 = 0.1914	R_1 = 0.1372, wR_2 = 0.2116
Largest diff. peak/hole / e Å-3	0.56/-0.40	0.57/-0.43	0.58/-0.42

Table S4. Crystallographic information for **SO_2@Cr_8_VT350K_1-4**

Identification code	**SO_2@Cr_8_VT350K_1**	**SO_2@Cr_8_VT350K_2**	**SO_2@Cr_8_VT350K_3**	**SO_2@Cr_8_VT350K_4**
Empirical formula	$C_{80}H_{144}Cr_8F_8O_{33.67}S_{0.83}$	$C_{80}H_{144}Cr_8F_8O_{33.08}S_{0.54}$	$C_{80}H_{144}Cr_8F_8O_{32.91}S_{0.46}$	$C_{80}H_{144}Cr_8F_8O_{33.08}S_{0.54}$
Formula weight	2239.45	2220.54	2220.54	2220.54
Temperature/K	249.9(5)	249.9(5)	240.0	239.76(10)
Crystal system	Monoclinic	monoclinic	monoclinic	monoclinic
Space group	I2/a	I2/a	I2/a	I2/a
a/Å	34.9035(10)	34.8692(12)	34.8538(12)	34.8442(12)
b/Å	16.6096(3)	16.6217(3)	16.6225(3)	16.6245(3)
c/Å	44.7863(12)	44.8285(12)	44.8355(13)	44.8378(13)
α/°	90	90	90	90
β/°	111.483(3)	111.414(4)	111.414(4)	111.392(4)
γ/°	90	90	90	90
Volume/Å^3	24160.3(11)	24188.4(13)	24182.6(13)	24183.7(13)
Z	8	8	8	8
ρ_{calc}g/cm^3	1.231	1.220	1.220	1.220
μ/mm^{-1}	0.781	0.775	0.775	0.775
F(000)	9366.0	9290.0	9290.0	9290.0
Crystal size/mm^3	0.5 × 0.1 × 0.1	0.5 × 0.1 × 0.1	0.5 × 0.1 × 0.1	0.5 × 0.1 × 0.1
Radiation	MoKα (λ = 0.71073)	MoKα (λ = 0.71073)	MoKα (λ = 0.71073)	MoKα (λ = 0.71073)
2Θ range for data collection/°	6.884 to 52.744	6.774 to 52.744	6.776 to 52.744	6.776 to 52.744
Index ranges	$-41 \le h \le 43$, $-20 \le k \le 20$, $-55 \le l \le 54$	$-40 \le h \le 43$, $-20 \le k \le 20$, $-56 \le l \le 55$	$-40 \le h \le 43$, $-20 \le k \le 20$, $-56 \le l \le 55$	$-40 \le h \le 43$, $-20 \le k \le 20$, $-56 \le l \le 55$
Reflections collected	73573	73346	73383	73308
Independent reflections	24445 [R_{int} = 0.0237, R_{sigma} = 0.0299]	24464 [R_{int} = 0.0272, R_{sigma} = 0.0359]	24460 [R_{int} = 0.0266, R_{sigma} = 0.0343]	24464 [R_{int} = 0.0271, R_{sigma} = 0.0348]
Data/restraints/parameters	24445/1013/1536	24464/1019/1536	24460/1019/1536	24464/1001/1536
Goodness-of-fit on F^2	1.047	1.044	1.030	1.053
Final R indexes [I>=2σ (I)]	R_1 = 0.0455, wR_2 = 0.1253	R_1 = 0.0465, wR_2 = 0.1258	R_1 = 0.0461, wR_2 = 0.1240	R_1 = 0.0464, wR_2 = 0.1259
Final R indexes [all data]	R_1 = 0.0627, wR_2 = 0.1347	R_1 = 0.0652, wR_2 = 0.1352	R_1 = 0.0658, wR_2 = 0.1338	R_1 = 0.0662, wR_2 = 0.1357
Largest diff. peak/hole / e Å^{-3}	0.57/-0.67	0.58/-0.63	0.56/-0.61	0.55/-0.63

Table S5. Crystallographic information for **SO_2@Cr_8_VT350K_5-7**

Identification code	**SO_2@Cr_8_VT350K_5**	**SO_2@Cr_8_VT350K_6**	**SO_2@Cr_8_VT350K_7**
Empirical formula	$C_{80}H_{144}Cr_8F_8O_{32.89}S_{0.45}$	$C_{80}H_{144}Cr_8F_8O_{32.89}S_{0.45}$	$C_{80}H_{144}Cr_8F_8O_{32.86}S_{0.43}$
Formula weight	2220.54	2214.43	2213.55
Temperature/K	239.9(5)	239.74(10)	240.0
Crystal system	monoclinic	monoclinic	monoclinic
Space group	I2/a	I2/a	I2/a
a/Å	34.8328(12)	34.8231(12)	34.8365(12)
b/Å	16.6255(3)	16.6250(3)	16.6328(3)
c/Å	44.8334(13)	44.8309(13)	44.8540(13)
α/°	90	90	90
β/°	111.373(4)	111.355(4)	111.361(4)
γ/°	90	90	90
Volume/Å^3	24178.0(13)	24172.2(13)	24204.3(13)
Z	8	8	8
ρ_{calc}g/cm^3	1.220	1.217	1.215
μ/mm^{-1}	0.775	0.773	0.772
F(000)	9290.0	9266.0	9262.0
Crystal size/mm^3	0.5 × 0.1 × 0.1	0.5 × 0.1 × 0.1	0.5 × 0.1 × 0.1
Radiation	MoKα (λ = 0.71073)	MoKα (λ = 0.71073)	MoKα (λ = 0.71073)
2Θ range for data collection/°	6.778 to 52.744	6.778 to 52.742	6.776 to 52.744
Index ranges	-40 ≤ h ≤ 43, -20 ≤ k ≤ 20, -56 ≤ l ≤ 55	-40 ≤ h ≤ 43, -20 ≤ k ≤ 20, -56 ≤ l ≤ 55	-40 ≤ h ≤ 43, -20 ≤ k ≤ 20, -56 ≤ l ≤ 55
Reflections collected	73304	73317	73435
Independent reflections	24466 [R_{int} = 0.0270, R_{sigma} = 0.0352]	24458 [R_{int} = 0.0268, R_{sigma} = 0.0347]	24503 [R_{int} = 0.0270, R_{sigma} = 0.0349]
Data/restraints/parameters	24466/1001/1536	24458/1001/1536	24503/1001/1536
Goodness-of-fit on F^2	1.055	1.037	1.040
Final R indexes [I>=2σ (I)]	R_1 = 0.0467, wR_2 = 0.1264	R_1 = 0.0466, wR_2 = 0.1269	R_1 = 0.0467, wR_2 = 0.1277
Final R indexes [all data]	R_1 = 0.0674, wR_2 = 0.1364	R_1 = 0.0666, wR_2 = 0.1368	R_1 = 0.0670, wR_2 = 0.1377
Largest diff. peak/hole / e Å^{-3}	0.59/-0.72	0.58/-0.61	0.58/-0.64

Table S6. Crystallographic information for **SO_2@Cr_8_VT400K_1-2**

Identification code	**SO_2@Cr_8_VT400K_1**	**SO2@Cr8_VT400K_2**
Empirical formula	$C_{80}H_{144}Cr_8F_8O_{33.73}S_{0.87}$	$C_{80}H_{144}Cr_8F_8O_{32}$
Formula weight	2241.44	2185.94
Temperature/K	240.0	240.0
Crystal system	monoclinic	monoclinic
Space group	I2/a	I2/a
a/Å	34.7891(14)	34.7214(11)
b/Å	16.5631(3)	16.5877(3)
c/Å	44.6159(18)	44.6977(17)
α/°	90	90
β/°	111.394(4)	111.193(4)
γ/°	90	90
Volume/Å^3	23936.9(16)	24002.4(14)
Z	8	8
ρ_{calc}g/cm^3	1.244	1.210
μ/mm^{-1}	0.789	0.770
F(000)	9374.0	9152.0
Crystal size/mm^3	0.5 × 0.1 × 0.1	0.4 × 0.1 × 0.1
Radiation	MoKα (λ = 0.71073)	MoKα (λ = 0.71073)
2Θ range for data collection/°	3.396 to 52.744	3.396 to 52.744
Index ranges	$-43 \leq h \leq 43$, $-16 \leq k \leq 20$, $-55 \leq l \leq 55$	$-43 \leq h \leq 43$, $-15 \leq k \leq 20$, $-55 \leq l \leq 55$
Reflections collected	66189	66712
Independent reflections	24468 [R_{int} = 0.0283, R_{sigma} = 0.0394]	24447 [R_{int} = 0.0263, R_{sigma} = 0.0354]
Data/restraints/parameters	24468/728/1461	24447/864/1491
Goodness-of-fit on F^2	1.048	1.051
Final R indexes [I>=2σ (I)]	R_1 = 0.0481, wR_2 = 0.1269	R_1 = 0.0499, wR_2 = 0.1418
Final R indexes [all data]	R_1 = 0.0719, wR_2 = 0.1373	R_1 = 0.0713, wR_2 = 0.1531
Largest diff. peak/hole / e Å^{-3}	0.56/-0.59	1.38/-0.40

Table S8. Variation of SO_2 occupancy with temperature in SO_2@1_M structures (M = 100, 150, 200, 250, 300 and 350K)

Table S7. Crystallographic information for **SO_2@Cr_8_hkl_350-400K**

Identification code	**SO_2@Cr_8_hkl_350K**	**SO_2@Cr_8_hkl_375K**	**SO_2@Cr_8_hkl_400K**
Empirical formula	$C_{80}H_{144}Cr_8F_8O_{33.66}S_{0.83}$	$C_{80}H_{144}Cr_8F_8O_{33.73}S_{0.86}$	$C_{80}H_{144}Cr_8F_8O_{33.76}S_{0.88}$
Formula weight	2239.09	2241.44	2242.32
Temperature/K	149.9(5)	149.8(5)	149.8(5)
Crystal system	monoclinic	monoclinic	monoclinic
Space group	I2/a	I2/a	I2/a
a/Å	34.7518(9)	34.8086(10)	34.7957(14)
b/Å	16.4960(3)	16.4934(3)	16.4957(3)
c/Å	44.0635(11)	44.0632(12)	44.1262(15)
α/°	90	90	90
β/°	111.433(3)	111.439(3)	111.360(4)
γ/°	90	90	90
Volume/Å^3	23513.2(11)	23546.8(11)	23587.8(15)
Z	8	8	8
ρ_{calc}g/cm^3	1.265	1.265	1.263
μ/mm^{-1}	0.803	0.802	0.801
F(000)	9364.0	9374.0	9377.0
Crystal size/mm^3	0.5 × 0.1 × 0.1	0.5 × 0.1 × 0.1	0.5 × 0.1 × 0.1
Radiation	MoKα (λ = 0.71073)	MoKα (λ = 0.71073)	MoKα (λ = 0.71073)
2Θ range for data collection/°	3.13 to 52.744	3.13 to 52.744	3.128 to 52.744
Index ranges	$-39 \le h \le 43$, $-20 \le k \le 20$, $-54 \le l \le 54$	$-38 \le h \le 43$, $-20 \le k \le 11$, $-55 \le l \le 43$	$-36 \le h \le 43$, $-20 \le k \le 18$, $-47 \le l \le 55$
Reflections collected	64959	61472	53902
Independent reflections	23939 [R_{int} = 0.0463, R_{sigma} = 0.0611]	24044 [R_{int} = 0.0410, R_{sigma} = 0.0580]	24071 [R_{int} = 0.0353, R_{sigma} = 0.0533]
Data/restraints/parameters	23939/1019/1536	24044/741/1461	24071/813/1461
Goodness-of-fit on F^2	1.058	1.042	1.045
Final R indexes [I>=2σ (I)]	R_1 = 0.0470, wR_2 = 0.1201	R_1 = 0.0474, wR_2 = 0.1152	R_1 = 0.0469, wR_2 = 0.1143
Final R indexes [all data]	R_1 = 0.0743, wR_2 = 0.1322	R_1 = 0.0703, wR_2 = 0.1245	R_1 = 0.0681, wR_2 = 0.1236
Largest diff. peak/hole / e Å^{-3}	0.71/-0.62	0.76/-0.68	0.80/-0.65

T/K	Position	Occupancy	Occupancy (%)	S-O bond lengths /Å		O-S-O bond angle/°
100	1	0.489(6) (56)	56	1.377(15)	1.483(15)	116.8(9)
	2	0.271(6) (31)	31	1.472(18)	1.415(19)	115.2(16)
	3	0.110(5) (13)	13	1.390(19)	1.402(18)	1.216(18)
150	1	0.424(6) (49)	49	1.380(16)	1.465(15)	115.9(11)
	2	0.300(6) (34)	34	1.472(18)	1.406(19)	113.8(15)
	3	0.143(5) (17)	17	1.386(18)	1.399(18)	120.0(18)
200	1	0.389(7) (44)	44	1.399(17)	1.471(17)	114.4(13)
	2	0.311(7) (35)	35	1.468(18)	1.411(18)	113.9(15)
	3	0.182(7) (21)	21	1.373(18)	1.389(19)	123(2)
250	1	0.335(9) (38)	38	1.474(18)	1.436(18)	109.7(15)
	2	0.320(8) (36)	36	1.444(19)	1.484(18)	108.7(14)
	3	0.227(8) (26)	26	1.394(18)	1.444(19)	114.1(17)
300	1	0.302(8) (36)	36	1.407(18)	1.441(19)	111.6(16)
	2	0.279(8) (33)	33	1.439(19)	1.443(18)	109.6(15)
	3	0.260(8) (31)	31	1.404(18)	1.433(18)	112.3(15)
310	1	0.271(9) (34)	34	1.422(19)	1.45(2)	110.2(17)
	2	0.270(9) (34)	34	1.448(19)	1.430(19)	109.6(16)
	3	0.246(8) (32)	32	1.420(18)	1.443(18)	110.5(16)
350	1	0.215(9) (34)	34	1.428(19)	1.45(2)	112.3(18)
	2	0.210(9) (33)	33	1.43(2)	1.449(19)	111.8(18)
	3	0.211(9) (33)	33	1.450(19)	1.439(19)	111.4(18)

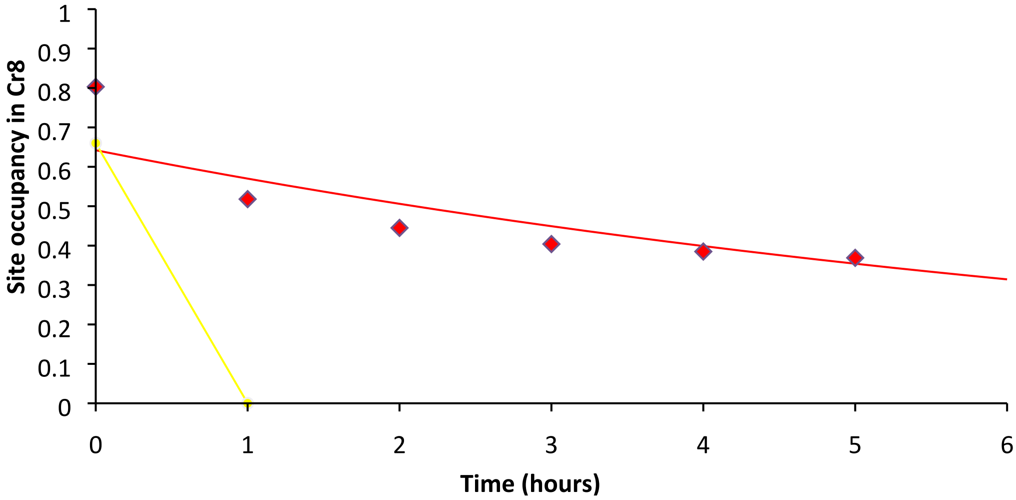

Figure S6. Site occupancy of molecules inside **Cr_8** vs heating time at 350 K, SO_2 shown as red diamonds, H_2S as yellow circles. The data for SO_2 release were fitted to an exponential decay, $y = 0.642\ e^{-0.119x}$, shown as red line with a R^2 of

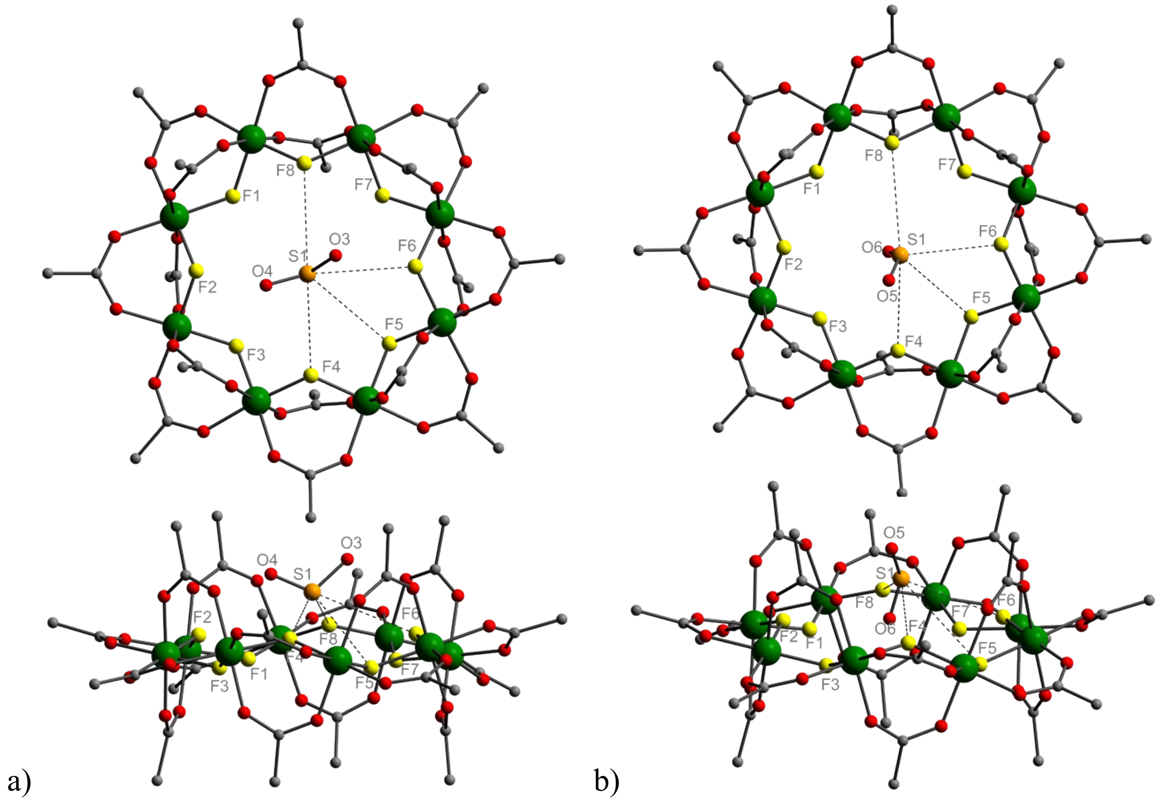

Figure S7. a) Second component (position 2) of the SO_2 disorder inside the cavity of $\mathbf{Cr_8}$, with 0.265 occupancy, and b) is the third component (position 3 with 0.102 occupancy

- **Activation energy determination from single crystal X-Ray Diffraction Experiments**

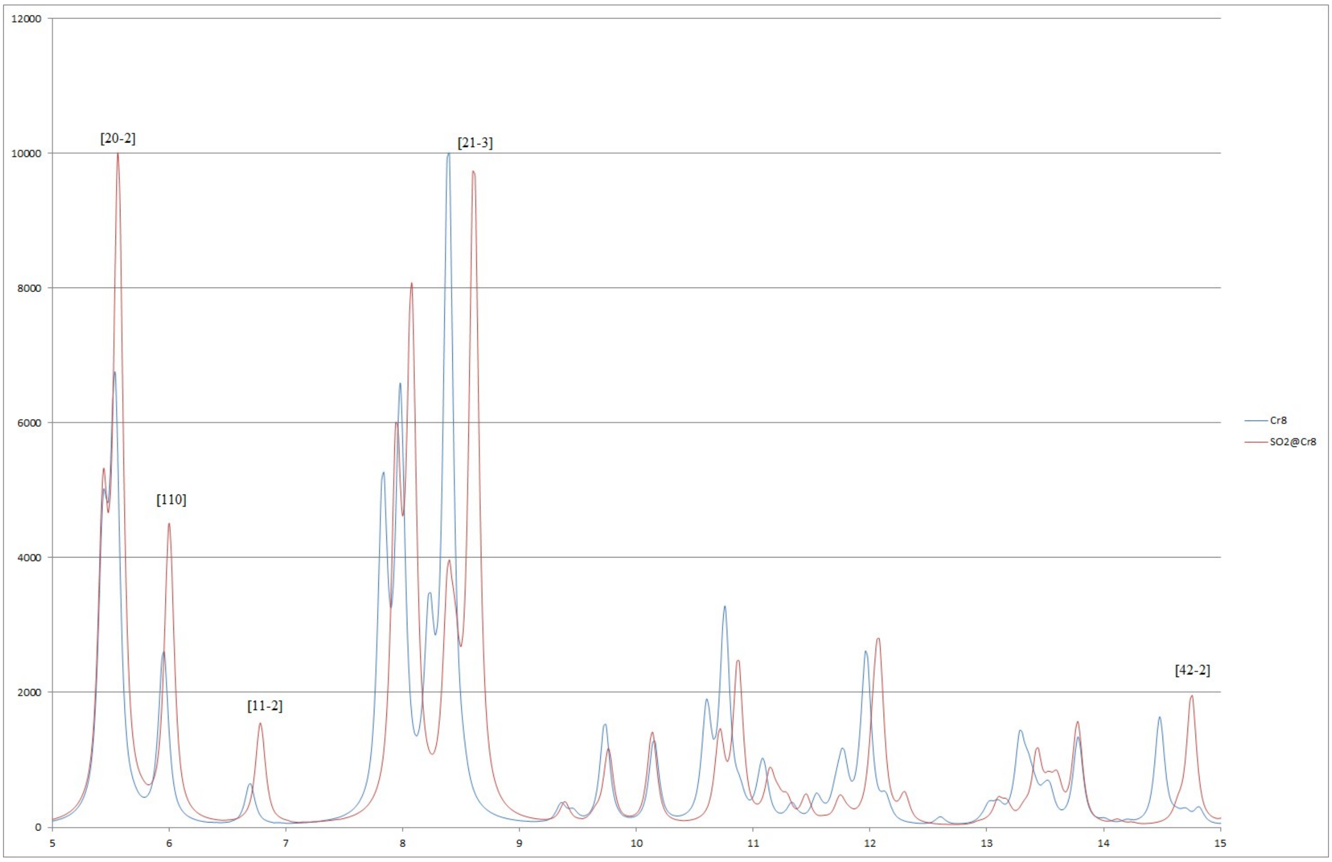

Figure S8. Simulated Powder XRD spectra for the **SO_2@Cr_8** (red) and **Cr_8** (blue) with the selected hkl planes

The experimental protocol comprised of the collection of a data set of **SO_2@Cr_8** at 150 K to confirm the starting structure, followed by the heating of the sample to 400, 375 and 350K and holding it at that temperature for 2, 4 and 8 hours whilst collecting short data sets with 2s per frame. The data was processed with 40.7b CrysAlisPro software package. Reflexions corresponding to [110] and [11-2] hkl planes were identified. Then, only frames containing the selected reflexions were monitored. The peak intensity was calculated plotting a one dimensional profile of the reflexion. The SO_2 release rates were calculated at three different temperatures (350, 375 and 400K) by exponential regression of the intensity/time progression of the hkl planes [110] and [11-2]. Linear regression on the calculated release rates obtained produced two activation energy values of 25.3 and 31 kJ/mol, which are very close to the activation energy determined through DSC analysis of 26 kJ/mol.

Table S9. Intensity decrease of [110] plane at 400K

Time (s) after reaching T=400K	Time (h) after reaching T=400K	Intensity – [110] plane
844	0.234	2144
1538	0.427	2055
2220	0.617	1849
2901	0.806	1846
3581	0.995	1675
4271	1.186	1626
4966	1.379	1584
5646	1.568	1677
6327	1.758	1566
7016	1.949	1574

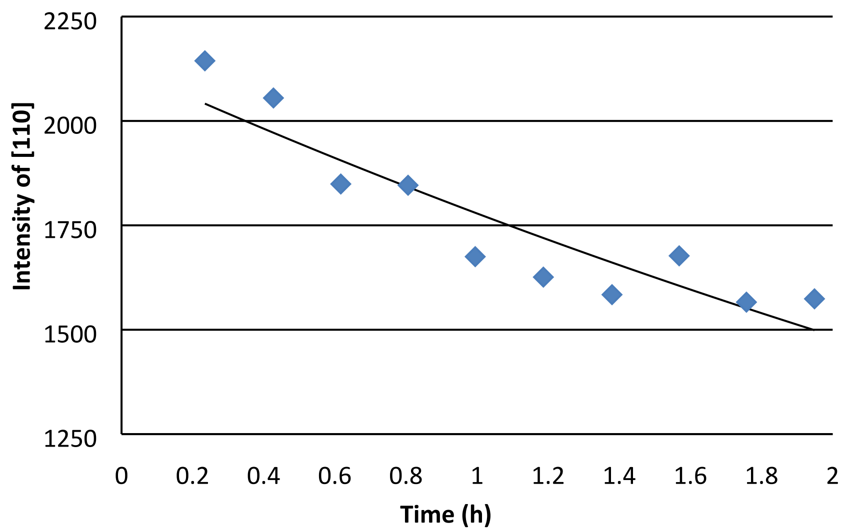

Figure S9. Intensity of [110] plotted over time, with exponential regression

Table S10. Intensity decrease of [11-2] plane at 400K

Time (s) after reaching T=400K	Time (h) after reaching T=400K	Intensity – [11-2] plane
769	0.214	19525
1463	0.406	17223
2145	0.596	16214
2825	0.785	15444
3505	0.974	14611
4196	1.166	14284
4891	1.359	13830
5571	1.548	13741
6251	1.736	13487
6941	1.928	13316

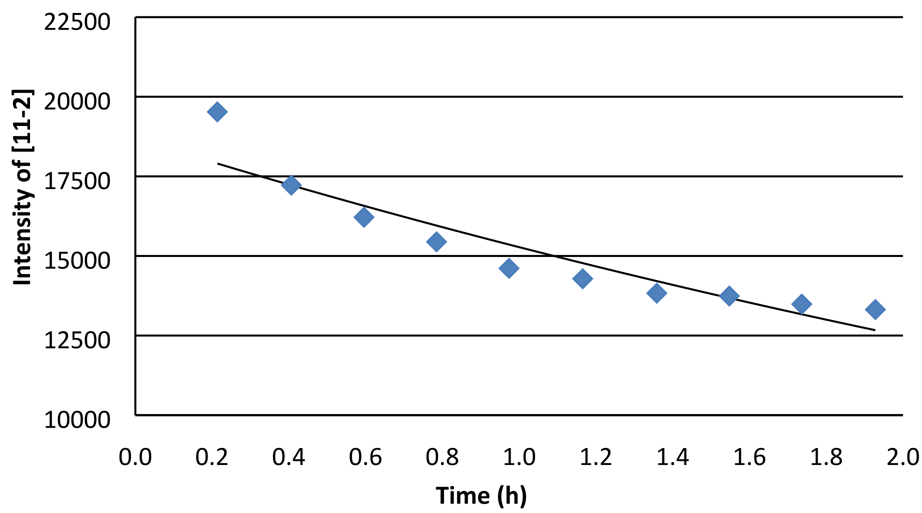

Figure S10. Intensity of [11-2] plotted over time, with exponential regression

Table S11. Intensity decrease of [110] plane at 375K

Time (s) after reaching T=375K	Time (h) after reaching T=375K	Intensity – [110] plane
800	0.222	13729
1589	0.441	10658
2355	0.654	11978
3125	0.868	11530
3894	1.082	11698
4673	1.298	11684
5445	1.513	11440
6211	1.725	10629
7003	1.945	10340
7773	2.159	10241
8542	2.373	10224
9352	2.598	10190
10300	2.861	10141
11101	3.084	9653
11871	3.298	9556
12640	3.511	9472
13407	3.724	9593
14177	3.938	9852

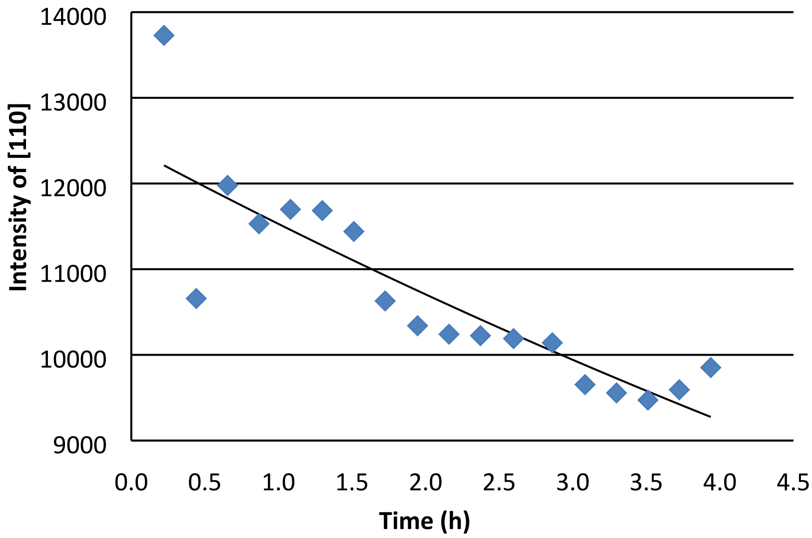

Figure S11. Intensity of [110] plotted over time, with exponential regression

Table S12. Intensity decrease of [11-2] plane at 375K

Time (s) after reaching T=375K	Time (h) after reaching T=375K	Intensity – [11-2] plane
644	0.179	44959
1433	0.398	51409
2197	0.610	49648
2966	0.824	47377
3736	1.038	45603
4514	1.254	43035
5287	1.469	40569
6053	1.681	39241
6844	1.901	36926
7615	2.115	36203
8394	2.332	34671
9194	2.554	33940
9962	2.767	32726
10762	2.989	31682
11533	3.204	31099
12302	3.417	30533
13069	3.630	29023
13839	3.844	29704

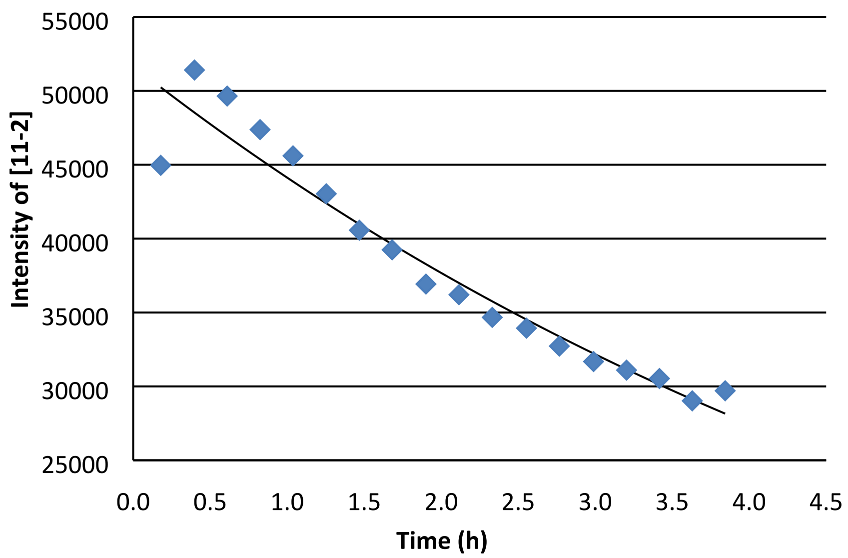

Figure S12. Intensity of [11-2] plotted over time, with exponential regression

Table S13. Intensity decrease of [110] plane at 350K

Time (s) after reaching T=350K	Time (h) after reaching T=350K	Intensity – [110] plane
883	0.245	66104
1777	0.494	62737
2665	0.74	59749
3558	0.988	58765
4448	1.236	56462
5331	1.481	54659
6230	1.731	53938
7122	1.978	52945
8005	2.224	51492
8889	2.469	50929
9777	2.716	50555
10660	2.961	49881
11547	3.208	49222
12446	3.457	48436
13329	3.703	48313
14221	3.95	47573
15104	4.196	47517
15986	4.441	47136
16870	4.686	46779
17770	4.936	46104
18653	5.181	45875
19538	5.427	46129
20421	5.673	45866
21303	5.918	44858
22155	6.154	44620
23060	6.406	45096
23942	6.651	43933
24824	6.896	44081
25708	7.141	44433
26591	7.386	44104
27527	7.646	42919

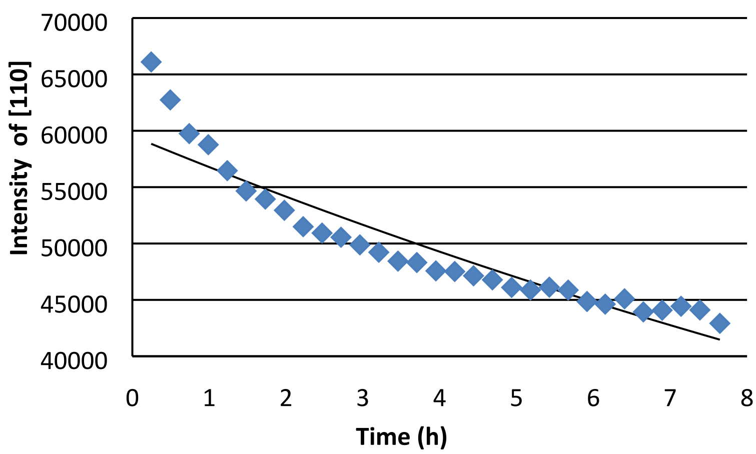

Figure S13. Intensity of [110] plotted over time, with exponential regression

Table S14. Intensity decrease of [11-2] plane at 350K

Time (s) after reaching T=350K	Time (h) after reaching T=350K	Intensity – [11-2] plane
953	0.265	28035
1849	0.514	26545
2737	0.76	25000
3630	1.008	24542
4520	1.256	23164
5403	1.501	22837
6302	1.751	22435
7194	1.998	21031
8077	2.244	20736
8961	2.489	20359
9849	2.736	19591
10732	2.981	19401
11619	3.228	18757
12518	3.477	18962
13401	3.723	18968
14293	3.97	17976
15176	4.216	17924
16058	4.461	17643
16942	4.706	17446
17842	4.956	17545
18725	5.201	17014
19610	5.447	16975
20493	5.693	17113
21375	5.938	16491
22227	6.174	16750
23132	6.426	16639
24014	6.671	16277
24896	6.916	16176
25780	7.161	16171
26663	7.406	15900
27559	7.655	15793

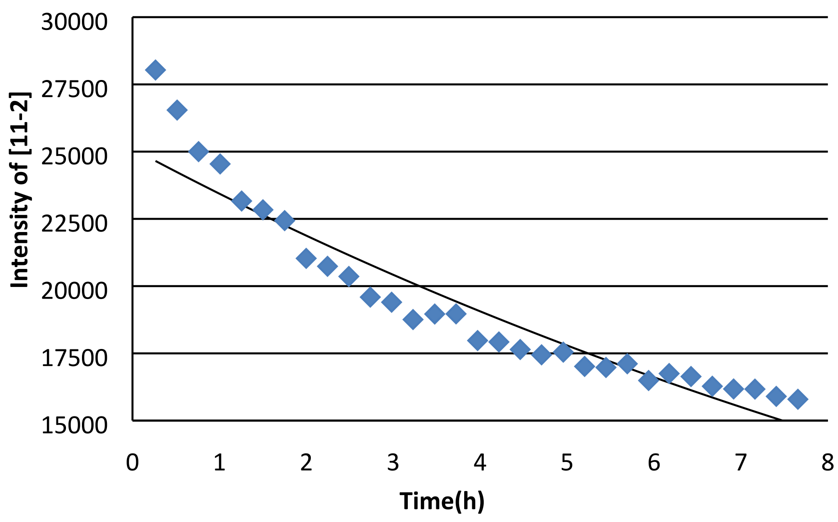

Figure S14. Intensity of [11-2] plotted over time, with exponential regression

Table S15. Release rates obtained from the regressions for the two planes and the averaged release rates

k (h^{-1})	[110]	[11-2]	average
400K	0.047	0.069	0.058
375K	0.074	0.158	0.116
350K	0.18	0.202	0.191

Table S16. Release rates table for plane [110]

T	1/T	k	lnk
350	0.0029	0.047	-3.0576
375	0.0027	0.074	-2.6037
400	0.0025	0.18	-1.7148

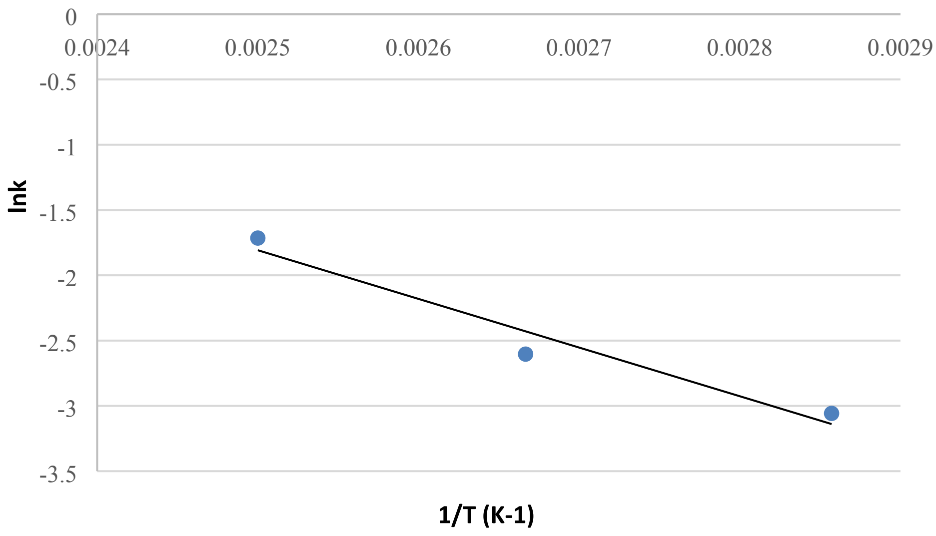

Figure S15. lnk vs 1/T for plane[110]

$-E_a/R = -3727.3$; $E_a = 31.0$ kJ/mol

Table S17. Release rates table for plane [11-2]

T	1/T	k	lnk
350	0.0029	0.069	-2.6736
375	0.0027	0.158	-1.8452
400	0.0025	0.202	-1.5995

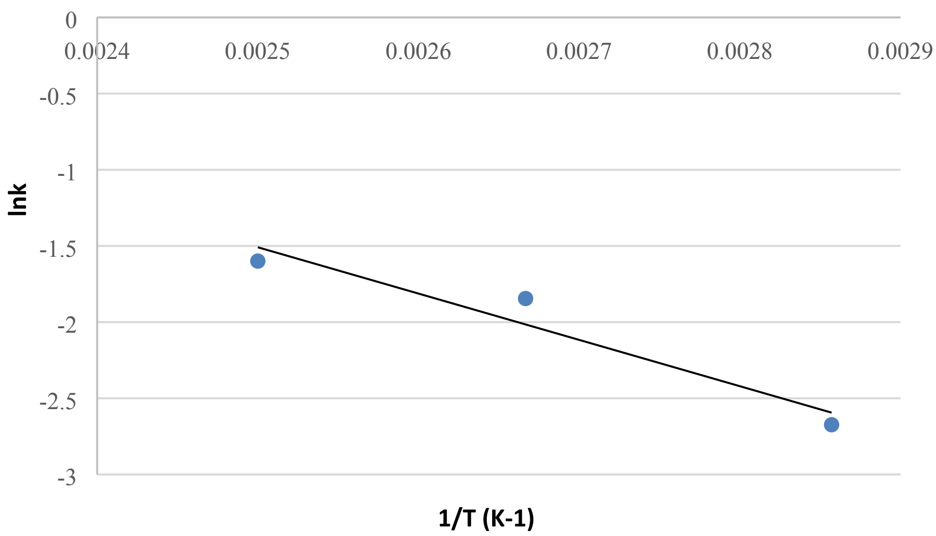

Figure S16. lnk vs 1/T for plane[11-2]

$-E_a/R$= -3039.4; E_a = 25.3 kJ/mol

Table S18. Averaged release rates table

T	1/T	avgK	lnavgk
350	0.0029	0.058	-2.8473
375	0.0027	0.116	-2.1542
400	0.0025	0.191	-1.6555

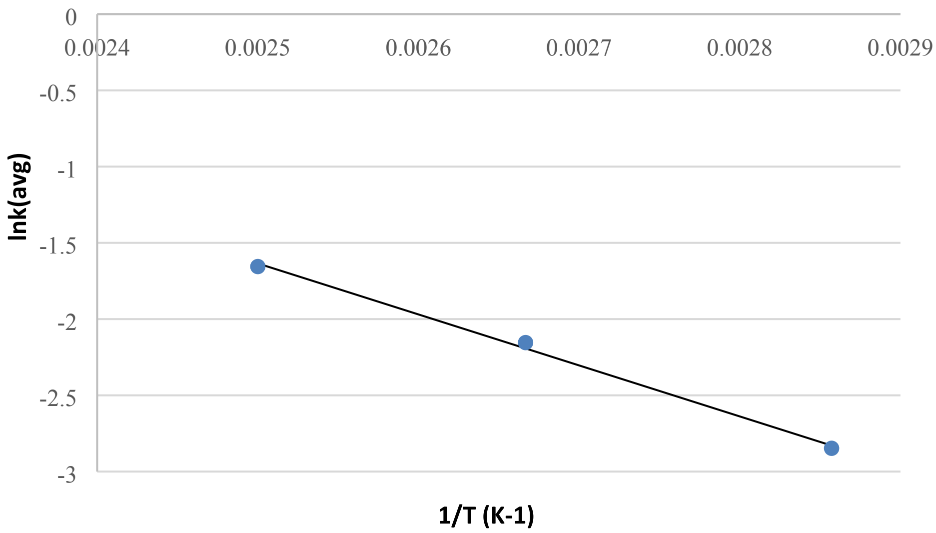

Figure S17. lnk vs 1/T for the averaged release rates

$-E_a/R$= -3344.3; E_a = 27.8 kJ/mol

S6. DFT calculations

Density functional theory (DFT) calculations within the Gaussian09 suite of programs[5] were used to investigate the structure of **SO_2@Cr_8** and **SH_2@Cr_8**. We employed the pure exchange-correlation PBE functional[6] with the Stuttgart RSC 1997 ECP pseudopotential[7] for chromium, and the basis sets cc-pVTZ[8] for O, S and F; cc-VDZ[9] for C and H. Empirical dispersion term (gd3)[10] were also accounted for.

We start from the lowest temperature crystal structure and select the atoms with the highest occupancy as a starting point for geometry optimisation. Given the complexity of the electronic structure of the Cr8 ring, we adopt the following procedure: i) a single-point calculation imposing a high-spin state at the crystal structure. ii) using these orbitals, we perform a restricted-optimisation where only the SO_2 and SH_2 is relaxed. iii) a sequential reduction of the spin multiplicity (from S=25 to S=1) permits describing the correct antiferromagnetic ground state with an appropriate broken symmetry solution. We note that the S=1 broken symmetry solution for **SO_2@Cr_8** does not show a complete alternant spin-up to spin-down distribution (Figure S18, right-panel), but we argue that the tiny energy difference involved (Table S19) will have no effect on the structure. iv) using the S=1 orbitals, we relax the position of the SO_2 and SH_2 again. Figures S18 and S19 compare the SO_2 and SH_2 positions in crystal, high-spin and low-spin states, respectively. These clearly indicate the good agreement between crystallographic and theoretical data. v) finally, we relax the whole structure. However, this might not be indicative of the experimental setup, as we are considering an isolated Cr_8 ring in gas phase which has no constrains to open up a bit to accommodate the gas molecules – in the solid state this is not feasible as the neighbouring molecules would prevent the breathing of the ring. Figures S20 and S21 compare the crystal and optimised **SO_2@Cr_8** and **SH_2@Cr_8** structures after overlapping them by minimising the root-mean square deviation values between the two structures, as proposed by Kabsch[11] and implemented by Kroman and Bratholm[12]. One can observe that in the case of SO_2, the molecule stays roughly in the same place as in the crystal. However, for the smaller SH_2, the ring expands a bit to allow for an encapsulation of the molecule, which drops to the centre of the ring. This is likely to be an artefact arising from neglecting the neighbouring molecules in the crystal lattice.

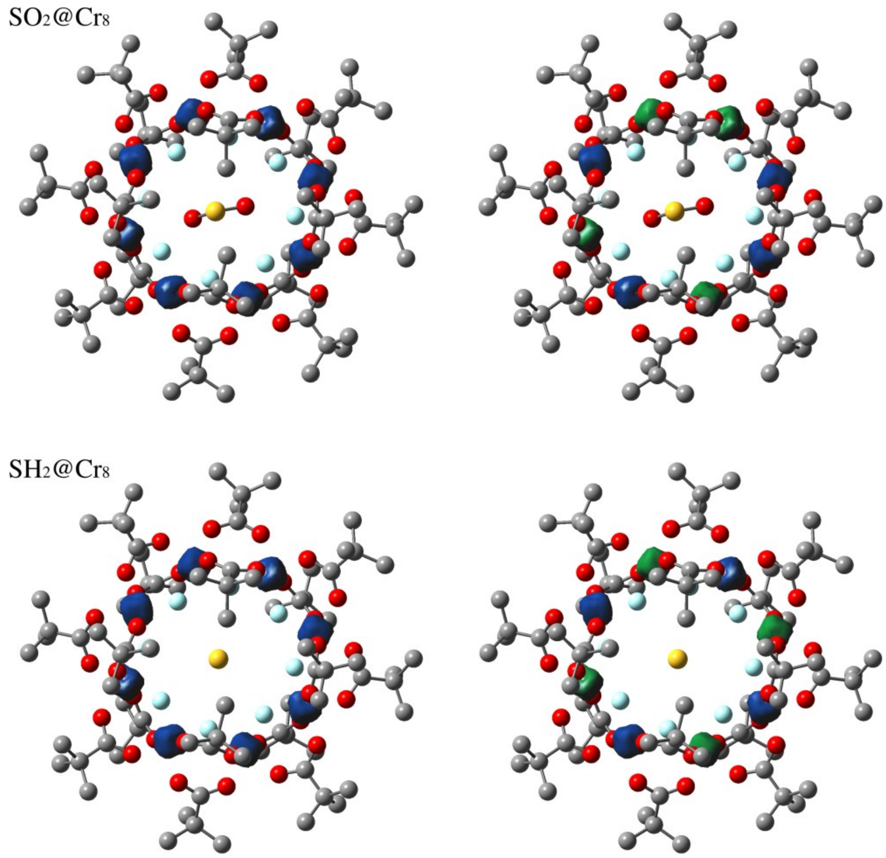

Figure S18. Spin density plots of $S = 25$ (left) and $S = 1$ (right) broken symmetry solutions for **SO_2@Cr_8** (up)and **SH_2@Cr_8** (bottom). Blue and green lobes indicate spin-up and spin-down densities, respectively.

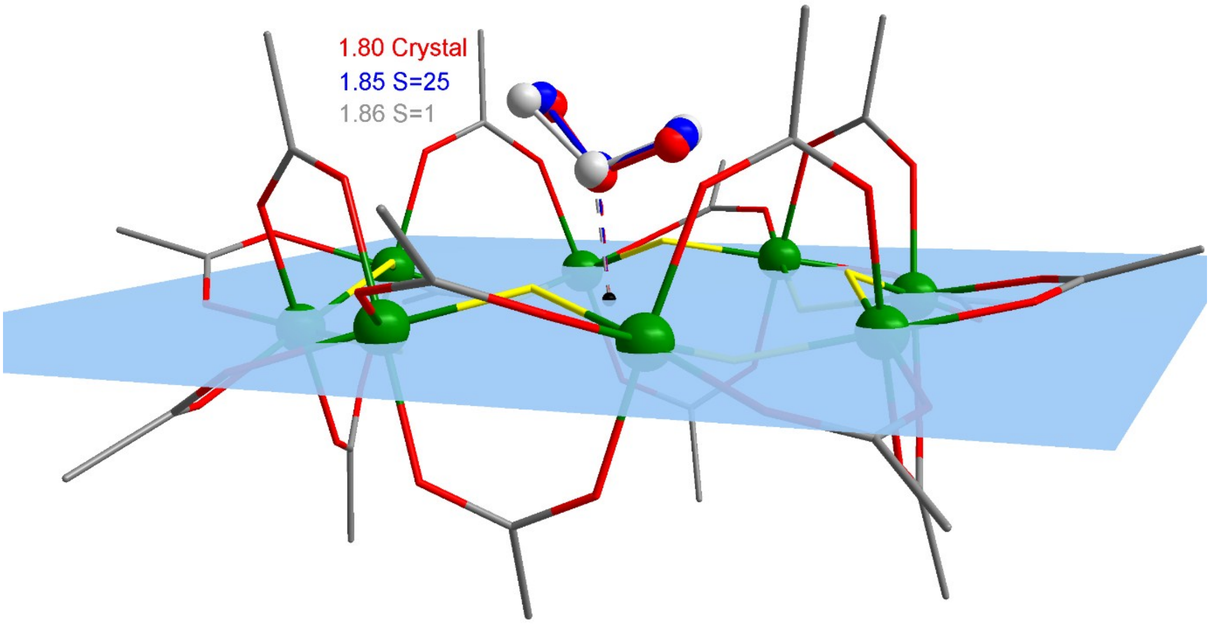

Figure S19. SO_2 position in the crystal (red), high-spin (blue) and low-spin (gray) fixed ring structures. Distance from sulfur atom to centroid of the Cr8 ring is highlighted.

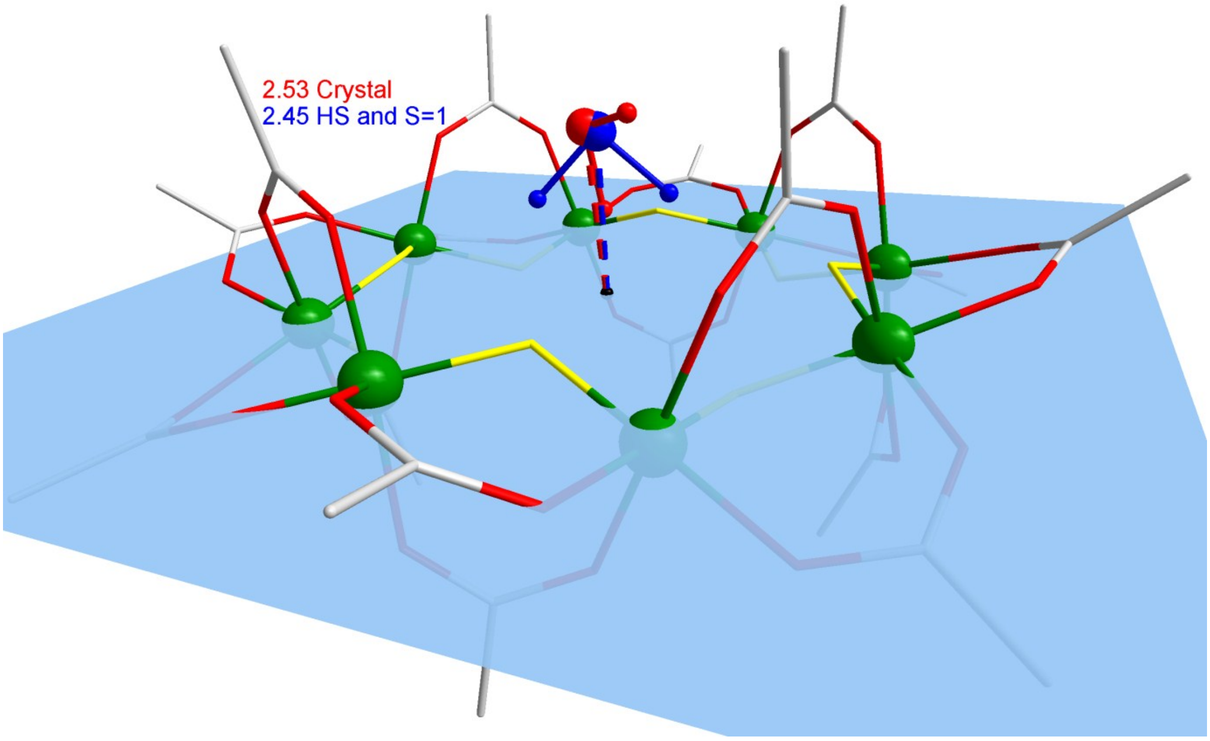

Figure S20. SH_2 position in the crystal (red), high-spin (blue) and low-spin (gray) fixed ring structures. Distance from sulfur atom to centroid of the Cr8 ring is highlighted.

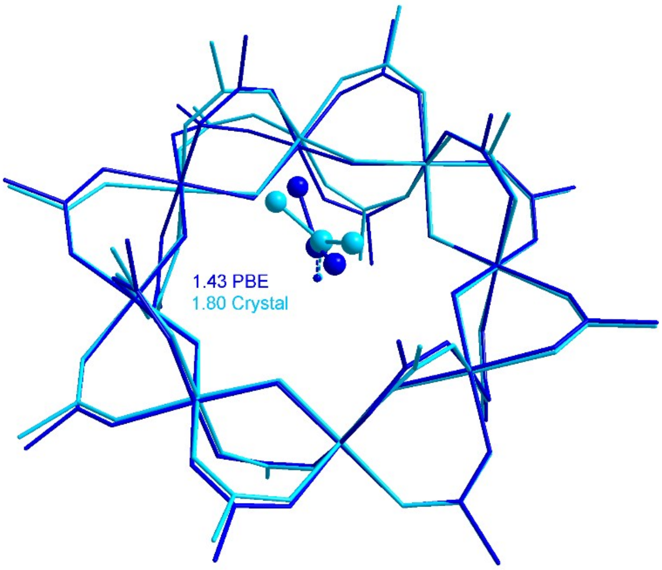

Figure S21. $SO_2@Cr_8$ structure comparison of crystal (pale blue) and optimised low-spin (dark blue). Distances from corresponding sulfur atom to centroid of the Cr8 ring are highlighted.

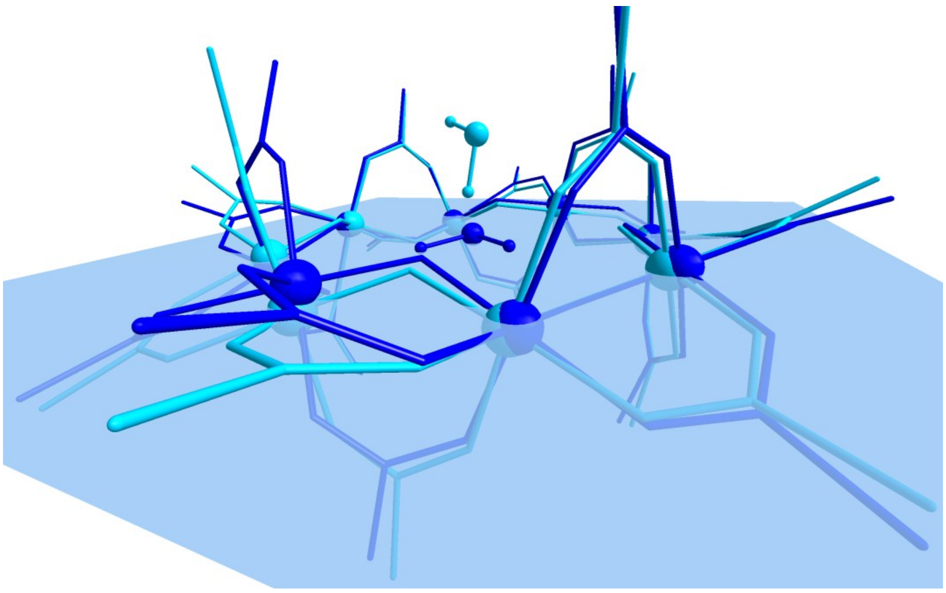

Figure S22. $SH_2@Cr_8$ structure comparison of crystal (pale blue) and optimised low-spin (dark blue).

Table S19. Summary of different broken symmetry solutions found.

$SO_2@Cr_8$

Multiplicity	Energy (hartree)	ΔE (cm-1)	Spin distribution Cr1 – Cr2 – Cr3 – Cr4 – Cr5 – Cr6 – Cr7 – Cr8
S = 25	-7579.2012		3/2 3/2 3/2 3/2 3/2 3/2 3/2 3/2
S = 23	-7579.1673	7432.0	1/2 3/2 3/2 3/2 3/2 3/2 3/2 3/2
S = 21	-7579.1669	7530.7	-1/2 3/2 3/2 3/2 3/2 3/2 3/2 3/2

S = 19	-7579.2024	-258.0	-3/2 3/2 3/2 3/2 3/2 3/2 3/2 3/2
S = 17	-7579.1682	7229.4	-3/2 1/2 3/2 3/2 3/2 3/2 3/2 3/2
S = 15	-7579.1664	7627.1	-3/2 -1/2 3/2 3/2 3/2 3/2 3/2 3/2
S = 13	-7579.2024	-276.6	-3/2 -3/2 3/2 3/2 3/2 3/2 3/2 3/2
S = 11	-7579.1683	7217.5	-3/2 -3/2 3/2 3/2 3/2 3/2 1/2 3/2
S = 9	-7579.1680	7281.8	-3/2 -3/2 3/2 3/2 3/2 3/2 -1/2 3/2
S = 7	-7579.2037	-547.6	-3/2 -3/2 3/2 3/2 3/2 3/2 -3/2 3/2
S = 5	-7579.1697	6897.2	-3/2 -3/2 3/2 3/2 1/2 3/2 -3/2 3/2
S = 3	-7579.1694	6982.0	-3/2 -3/2 3/2 3/2 -1/2 3/2 -3/2 3/2
S = 1	-7579.2049	-825.7	-3/2 -3/2 3/2 3/2 -3/2 3/2 -3/2 3/2

SH_2@Cr_8

Multiplicity	Energy (hartree)	ΔE (cm-1)	Spin distribution Cr1 – Cr2 – Cr3 – Cr4 – Cr5 – Cr6 – Cr7 – Cr8
S = 25	-7430.7133		3/2 3/2 3/2 3/2 3/2 3/2 3/2 3/2
S = 23	-7430.6795	7401.8	3/2 3/2 3/2 3/2 3/2 3/2 3/2 1/2
S = 21			
S = 19	-7430.7145	-265.3	3/2 3/2 3/2 3/2 3/2 3/2 3/2 -3/2
S = 17	-7430.6806	7167.6	3/2 3/2 3/2 1/2 3/2 3/2 3/2 -3/2
S = 15	-7430.6802	7253.8	3/2 3/2 3/2 -1/2 3/2 3/2 3/2 -3/2
S = 13	-7430.7157	-545.1	3/2 3/2 3/2 -3/2 3/2 3/2 3/2 -3/2
S = 11	-7430.6816	6938.7	3/2 3/2 3/2 -3/2 3/2 1/2 3/2 -3/2
S = 9	-7430.6813	7016.3	3/2 3/2 3/2 -3/2 3/2 -1/2 3/2 -3/2
S = 7	-7430.7170	-813.6	3/2 3/2 3/2 -3/2 3/2 -3/2 3/2 -3/2
S = 5	-7430.6827	6704.0	3/2 1/2 3/2 -3/2 3/2 -3/2 3/2 -3/2
S = 3	-7430.6827	6697.8	3/2 -1/2 3/2 -3/2 3/2 -3/2 3/2 -3/2
S = 1	-7430.7183	-1105.4	3/2 -3/2 3/2 -3/2 3/2 -3/2 3/2 -3/2

S7. References

1. I. J. Vitórica-Yrezábal, D. F. Sava, G. A. Timco, M. S. Brown, M. Savage, H. G. W. Godfrey, F. Moreau, M. Schröder, F. Siperstein, L. Brammer, S. Yang, M. P. Attfield, J. J. W. McDouall and R. E. P. Winpenny, *Angew. Chem. Int. Ed.*, 2017, **56**, 5527-5530

2. O.V. Dolomanov, L.J. Bourhis, R.J. Gildea, J.A.K. Howard, H. Puschmann, *J. Appl. Crystallogr.* 2009;**42(2)**, 339-341.

3. G. Sheldrick, *Acta Cryst. C.,* 2015;**71(1)**, 3-8.

4. D.R. Allan, W.G. Marshall, D.J. Francis, I.D.H. Oswald, C.R. Pulham, C. Spanswick, *Dalton Trans.*, 2010, **39(15)**, 3736-3743.

5. Gaussian 09, Revision D, M. J. Frisch et al., Gaussian, Inc., Wallingford CT, (2016).

6. a) Perdew, J. P.; Burke, K.; Ernzerhof, M. Generalized Gradient Approximation Made Simple. Phys. Rev. Lett. 77, 3865–3868 (1996). b) Perdew, J. P.; Burke, K.; Ernzerhof, M. Errata: Generalized Gradient Approximation Made Simple Phys. Rev. Lett. 78, 1396–1396 (1997).

7. a) Bergner, A., Dolg, M., Küchle, W., Stoll, H. & Preuß, H. Ab initio energy-adjusted pseudopotentials for elements of groups 13–17. Mol. Phys. 80, 1431–1441 (1993). b) Kaupp, M., Schleyer, P. v. R., Stoll, H. & Preuss, H. Pseudopotential approaches to Ca, Sr, and Ba hydrides. Why are some alkaline earth MX2 compounds bent? J. Chem. Phys. 94, 1360–1366 (1991). c) Dolg, M., Stoll, H., Preuss, H. & Pitzer, R. M. Relativistic and correlation effects for element 105 (hahnium, Ha): a comparative study of M and MO (M = Nb, Ta, Ha) using energy-adjusted ab initio pseudopotentials. J. Phys. Chem. 97, 5852–5859 (1993).

8. D.E. Woon and T.H. Dunning, Jr. J. Chem. Phys. 100, 2975 (1994).

9. Woon, D. E. & Dunning, T. H. Gaussian basis sets for use in correlated molecular calculations. III. The atoms aluminum through argon. J. Chem. Phys. 98, 1358–1371 (1993).

10. Grimme, S. Density functional theory with London dispersion corrections. Wiley Interdiscip. Rev. Comput. Mol. Sci. 1, 211–228 (2011).

11. a) W. Kabsch, IUCr, A solution for the best rotation to relate two sets of vectors, Acta Crystallogr. Sect. A 32 (1976) 922e923. b) W. Kabsch, IUCr, A discussion of the solution for the best rotation to relate two sets of vectors, Acta Crystallogr. Sect. A 34 (1978) 827e828.

12. J.C. Kroman, A. Bratholm, GitHub: Calculate RMSD for two XYZ structures. http://github.com/charnley/rmsd, 2016